Conclusions: On the basis of our initial analysis, we conclude that the observed pattern of volcanic features may be correlated with the distribution pattern of global physiographic and geologic characteristics. The distribution of volcanic centers and regional tectonic patterns suggests that volcanic features are generally excluded from lowlands and regions of tectonic shortening, and occur predominantly in upland regions characterized by geologic evidence for extension. Three hypotheses that may account for the observed distribution and geologic association may be categorized as (1) environment/elevation-related, (2) mantle dynamics-related, and (3) age-related. It is likely that all three influences occur, but on the basis of the global association of areas of high volcanic center abundance with tectonic characteristics of extension and the probable association of many individual volcanic centers with local mantle upwelling and plumes, we believe that the regional concentrations of volcanic centers may be primarily associated with regions of broad mantle upwelling phenomena. Although the broad-scale characteristics and association of the distribution of volcanic centers may be accounted for by the first hypothesis, details of the distribution and local associations may be strongly influenced by altitude and age-dependent effects.

References: [1] Bindschadler et al. (1990) *GRL, 17*, 1345. [2] Campbell et al. (1989) *Science, 246*, 373. [3] Crumpler et al. (1986) *Geology, 14*, 1031. [4] Crumpler et al. (1992) in preparation. [5] Grimm and Phillips (1991) *JGR, 96*, 8305. [6] Head et al. (1991) *GRL, 17*, 11337. [7] Head et al. (1991) *JGR*, submitted. [8] Head J. W. (1990) *Geology, 18*, 99. [9] Ivanov et al. (1992) *LPSC XXIII*. [10] Janes et al. (1992) *JGR*, submitted. [11] Kieffer and Hagar (1991) *JGR, 96*, 20967. [12] Lenardic et al. (1991) *GRL, 18*, 2209–2212. [13] Michaels et al. (1992) *LPSC XXIII*, 903. [14] Phillips et al. (1992) *JGR*, submitted. [15] Phillips et al. (1991) *Science, 252*, 651. [16] Pronin A. A. (1986) *Geotectonics, 20*, 271. [17] Roberts et al. (1991) *GRL, 17*, 1341. [18] Saunders et al. (1992) *JGR*, submitted. [19] Schaber et al. (1992) *JGR*, submitted. [20] Senske et al. (1992) *JGR*, submitted. [21] Senske and Head (1992) *LPSC XXIII*, 1269. [22] Squyres et al. (1992a) *JGR*, submitted. [23] Squyres et al. (1992b) *JGR*, submitted. [24] Stofan et al. (1992) *JGR*, submitted. [24] Stofan et al. (1991) *JGR, 96*, 20933. [25] Vorder Bruegge and Head (1989) *GRL, 16*, 699. [26] Head and Wilson (1992) *JGR, 97*, 3877. [27] Zuber (1990) *GRL, 17*, 1369–1372.

522-91 494917 **N93-14310**

THE SPIN VECTOR OF VENUS DETERMINED FROM MAGELLAN DATA.

M. E. Davies[1], T. R. Colvin[1], P. G. Rogers[1], P. W. Chodas[2], and W. L. Sjogren[2], [1]RAND, USA, [2]Jet Propulsion Laboratory, California Institute of Technology, Pasadena CA 91109, USA.

A control network of the north polar region of Venus has been established by selecting and measuring control points on full-resolution radar strips. The measurements were incorporated into a least-squares adjustment program that improved initial estimates of the coordinates of the control points, pole direction, and rotation rate of Venus. The current dataset contains 4206 measurements of 606 points on 619 radar strips. The accuracy of the determination is driven by spacecraft ephemeris errors. One method used to remove ephemeris errors is to adjust the averaged orbital inclination and argument of periapsis for each orbit. A more accurate method that has been used with selected blocks of orbits incorporates optimally fitting measurements of additional points at all latitudes of the radar strips together with Earth-based spacecraft radiometric tracking measurements to compute new spacecraft ephemerides. The root-mean-space (RMS) of the point measurement residuals in these improved ephemeris solutions is typically about 20 m in slant range, and 40 m in the along-track direction. Both the control network computations and the improved ephemeris solutions incorporate radii at the measured points derived from the Magellan altimetry dataset [1]. The radii of points north of 85° are computed in the least-squares adjustments.

An accurate estimate of the rotation period of Venus was obtained by applying the ephemeris improvement technique to the second cycle closure orbits 2166–2171 that overlaid the first cycle initial orbits 376–384. Sixty-four common points were measured on both orbit groups and improved ephemeris solutions computed over both blocks simultaneously, along with the rotation rate. A similar analysis was made using orbits 874–878 from cycle 1 and 4456–4458 from cycle 3. Fifty-two common points were measured on both orbit groups and the rotation period of 243.0185 ± 0.0001 was computed. This latter solution confirmed the initial solution, and was an improvement over the first closure solution because of the longer period between overlapping orbits.

The geodetic control network uses measurements of points on overlapping radar strips that cover the north polar region; these are only the even-numbered orbits. These strips were taken in the first cycle and encircle the pole except for three gaps due to the superior conjunction data loss, the reduced data due to occultation, and the area of ongoing work. Improved ephemeris solutions for 40 orbits (376–384, 520–528, 588–592, 658–668, 1002–1010, 1408–1412, 1746–1764, and 2166–2170) are included and fixed in the geodetic control computations, thus tying the network to the J2000 coordinate system. The argument of periapsis and orbital inclination of all remaining orbits were allowed to vary as part of the least-squares adjustment. The RMS of the point measurements is typically on the order of 75 m in both along-track and cross-track. The rotation period was fixed at 243.0185 days. The coordinates of the 606 measured points were determined and the solution for the direction of the north pole was $\alpha = 272.76° \pm 0.02°$, $\delta = 67.16° \pm 0.01°$ (J2000).

References: [1] Ford P. G. and Pettengill G. H. (1992) *JGR*, in press.

522-91 494918 **N93-14311**

MONTE CARLO COMPUTER SIMULATIONS OF VENUS EQUILIBRIUM AND GLOBAL RESURFACING MODELS.

D. D. Dawson[1], R. G. Strom[1], and G. G. Schaber[2], [1]University of Arizona, Tucson AZ 85721, USA, [2]U.S. Geological Survey, Flagstaff AZ 86001, USA.

Two models have been proposed for the resurfacing history of Venus: (1) equilibrium resurfacing and (2) global resurfacing. The equilibrium model [1] consists of two cases: In case 1 areas ≤0.03% of the planet are spatially randomly resurfaced at intervals of ≤150,000 yr to produce the observed spatially random distribution of impact craters and average surface age of about 500 m.y., and in case 2 areas ≥10% of the planet are resurfaced at intervals of ≥50 m.y. The global resurfacing model [2] proposes that the entire planet was resurfaced about 500 m.y. ago, destroying the preexisting crater population and followed by significantly reduced volcanism and tectonism. The present crater population has accumulated since then, with only 4% of the observed craters having been embayed by more recent lavas.

To test the equilibrium resurfacing model we have run several Monte Carlo computer simulations for the two proposed cases. For case 1 we used a constant resurfacing area of 0.03% of the planet with a constant thickness and a constant 150,000-yr time interval

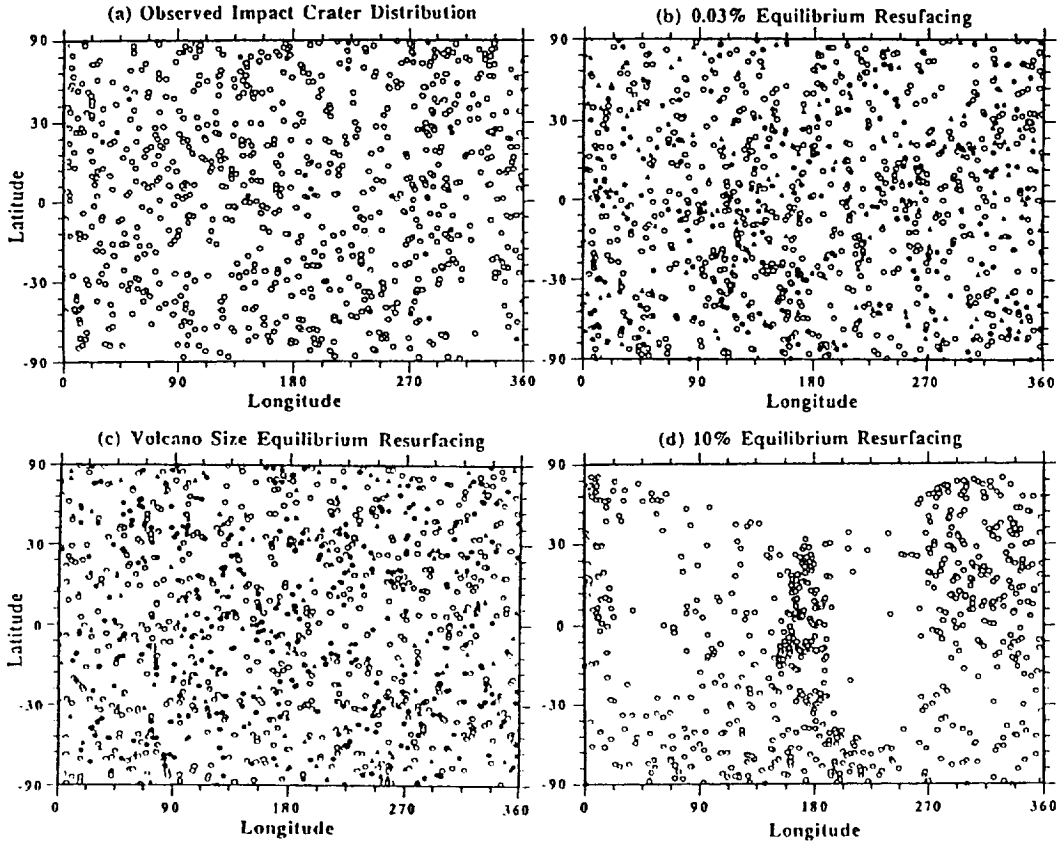

Fig. 1. (a) Observed Venus impact crater distribution. (b) 0.03% planet equilibrium resurfacing Monte Carlo simulation. (c) Observed volcano size distribution equilibrium resurfacing Monte Carlo simulation. (d) 10% equilibrium resurfacing Monte Carlo simulation. The unfilled circles are pristine craters, the solid circles are flooded craters, and the solid triangles are possibly flooded craters. Flooded craters not shown in (d).

between resurfacing events. Another more realistic simulation used the observed size distribution of volcanic features determined by Head et al. [3] and a variable time interval between resurfacing events that depended on the size of the event. Each simulation was run for a simulation period of 3 b.y. We took into account ejecta blankets by doubling the size of the craters. The center of each crater was marked with a dot, and the amount of the crater covered by resurfacing events was determined. Craters that were entirely covered by a single resurfacing event were considered destroyed. The minimum amount of flooded craters were those craters that had either not had their central point covered or had not had an area equal to 100% of their area covered. The maximum amount of flooded craters included the minimum amount and those craters that fulfilled both of the above criteria but had not been entirely covered by a single event. Some fraction of these latter craters may have been destroyed, but the others were probably intact and flooded. In fact, this category of crater only constituted about 15% of the total number of craters remaining after the simulations. Furthermore, a constant thickness resurfacing event is unrealistic and will produce more destroyed craters than a more realistic tapered event that will produced more partially flooded craters. For each simulation the input crater size-frequency distribution was the observed differential –0.2 slope for craters between 2 and 30 km diameter and the observed differential –3 slope at diameters greater than 30 km. After the simulations, however, the size distribution had changed to a –2 slope at diameters greater than 30 km, because over the simulation time of 3 b.y. the smaller craters were preferentially erased relative to the large craters to produce the –2 slope. Therefore, it was necessary to input an artificial size-frequency distribution with a –4 slope for craters greater than 30 km diameter in order to arrive at a –3 slope at the end of the simulation.

For the case 1 equilibrium resurfacing model to be valid the resulting crater distribution should be spatially random and there should be only about 4% partially flooded craters. Figures 1b and 1c show the results of the simulations compared to the observed crater distribution (Fig. 1a). Although the crater spatial distribution appears to be random, the amount of flooded craters is a minimum of 24% and maximum of 40% in the 0.03% resurfacing model, and a minimum of 30% and maximum of 46% in the more realistic observed volcano size distribution model. This is between 6 and 10 times the amount of flooded craters observed. The computer simulations do not take into account the more than 300 splotches that are part of the impact record and are not embayed by lava. This would only exacerbate the problem by producing many more flooded impact events. Furthermore, the input size frequency distribution above 30 km diameter required to produce the observed distribution

is completely unlike any size distribution on the terrestrial planets. Therefore, the computer simulations strongly indicate that the case 1 equilibrium resurfacing model is not a valid explanation for the resurfacing history of Venus. The observed nonrandom distribution of volcanic features [3] and the noncorrelation of the density of impact craters and volcanic features in equal areas [2] are further arguments against the equilibrium resurfacing model.

Case 2 of the equilibrium resurfacing model (≥10% resurfacing areas) simply will not work, except at the 100% (global) resurfacing level. Figure 1d is a Monte Carlo simulation for constant 10% resurfacing areas with a constant 50-m.y. time interval between events. Clearly the crater distribution is completely nonrandom and totally different from the observed distribution. We have done simulations for 25% and 50% resurfacing areas with similar results. Therefore, the equilibrium resurfacing model is not a valid model for an explanation of the observed crater population characteristics or Venus' resurfacing history.

The global resurfacing model is the most likely explanation for the characteristics of Venus' cratering record. The amount of resurfacing since that event, some 500 m.y. ago, can be estimated by a different type of Monte Carlo simulation. In this simulation the cratering record begins 500 m.y. ago with the observed crater size distribution. Our first simulation randomly selects craters from this size distribution and resurfaces areas with volcanos randomly selected from the observed volcano size distribution. The time interval between volcanic events is chosen so that only 4% of the craters are flooded at the end of 500 m.y. To date, our initial simulation has only considered the easiest case to implement. In this case the volcanic events are randomly distributed across the entire planet and, therefore, contrary to observation, the flooded craters are also randomly distributed across the planet. This simulation results in a maximum resurfaced area of about 10% of the planet since the global event, and an obliteration of about 4% of the craters. Future simulations will take into account the observed nonrandom distribution of flooded craters and, therefore, the nonrandom distribution of volcanic events. These simulations will probably result in a lower percentage of planet resurfacing because volcanism will be concentrated in smaller areas.

References: [1] Phillips R. J. et al. (1992) *LPSC XXIII*, 1065–1066. [2] Schaber G. G. et al. (1992) *JGR*, special Magellan issue, in press. [3] Head J. W. et al. (1992) *JGR*, special Magellan issue, in press.

N93-14312

METHANE MEASUREMENT BY THE PIONEER VENUS LARGE PROBE NEUTRAL MASS SPECTROMETER. T. M. Donahue[1] and R. R. Hodges Jr.[2], [1]University of Michigan, Ann Arbor MI 48109, USA, [2]University of Texas at Dallas, Richardson TX, 75083, USA.

The Pioneer Venus Large Probe Mass Spectrometer detected a large quantity of methane as it descended below 20 km in the atmosphere of Venus. Terrestrial methane and ^{136}Xe, both originating in the same container and flowing through the same plumbing, were deliberately released inside the mass spectrometer for instrumental reasons. However, the ^{136}Xe did not exhibit behavior similar to methane during Venus entry, nor did CH_4 in laboratory simulations. The CH_4 was deuterium poor compared to Venus water and hydrogen. While the inlet to the mass spectrometer was clogged with sulfuric acid droplets, significant deuteration of CH_4 and its H_2 progeny was observed. Since the only source of deuterium identifiable was water from sulfuric acid, we have concluded that we should correct the HDO/H_2O ratio in Venus water from 3.2×10^{-2} to $(5 \pm 0.7) \times 10^{-2}$.

When the probe was in the lower atmosphere, transfer of deuterium from Venus HDO and HD to CH_4 can account quantitatively for the deficiencies recorded in HDO and HD below 10 km, and consequently, the mysterious gradients in water vapor and hydrogen mixing ratios we have reported. The revision in the D/H ratio reduces the mixing ratio of water vapor (and H_2) reported previously by a factor of 3.2/5.

We are not yet able to say whether the methane detected was atmospheric or an instrumental artifact. If it was atmospheric, its release must have been episodic and highly localized. Otherwise, the large D/H ratio in Venus water and hydrogen could not be maintained.

N93-14313

VISCOELASTIC RELAXATION OF VENUSIAN CORONAE AND MOUNTAIN BELTS: CONSTRAINTS ON GLOBAL HEAT FLOW AND TECTONISM. J. Duncan and A. Leith, Department of Earth and Planetary Science, Washington University, St. Louis MO 63130, USA.

Venus differs from Earth in that water is essentially absent and its surface temperatures are about 470 K higher. The competing effects of high surface temperature and dry lithologies on the long-term history of surface topography have been studied using the finite-element method (Tecton) [1].

The relaxation history of surface topographic features, such as coronae and mountain belts, is a function of thermal gradient, crustal thickness and lithology, regional stresses, and basal tractions applied to the lithosphere. In this study we have examined the relative effects of these factors over a period of 500 Ma (presumed to be the mean age of the venusian surface) [2].

We assume that the venusian crust is composed of various combinations of diabase, gabbro, komatiite, and refractory lithologies such as anorthosite and websterite. Using appropriate thermal conductivities and surface heat fluxes scaled from Earth values (with and without a secular cooling contribution from the core) [3,4], thermal gradients ranging from about 20 K km^{-1} to 60 K km^{-1} are computed. We further assume that the thickness of a diabase crust is limited by the dry solidus. The models are dynamically isostatically balanced, using an elastic foundation.

Preliminary results of the study are shown in Fig. 1, in which a 2-km-high volcanic plateau has been instantaneously emplaced on the surface. For this model the crustal thermal gradient was 28 K km^{-1}. After the elastic response (essentially representing initial isostatic balance) the topography relaxes until the plateau is about 230 m above the surrounding region, and the slope from ridge crest to moat has been reduced from an initial 6° to about 2.5°. The values we obtain for our model plateau heights and slopes are in the observed range for venusian coronae. Thus we argue that coronae on Venus can be modeled as the product of elastoviscous relaxation of volcanic plateau. Although our starting models are oversimplifications, they do show all the critical morphological characteristics of venusian coronae. Matching the observed spectrum of corona morphology by varying the size, initial slope, and rheology of model plateaus enables constraints to be placed on plausible values for the venusian heat flux. We argue that the mean global heat flux must be significantly lower (~1/3) to be consistent with the observed spectrum of coronae topography.

We are presently examining models similar to those described above to investigate venusian mountain belts. Our models differ